Journal of
MATERIALS RESEARCH

Hydroxyapatite coatings grown by pulsed laser deposition with a beam of 355 nm wavelength

J.M. Fernández-Pradas,[a] L. Clèries, G. Sardin, and J.L. Morenza
Universitat de Barcelona, Departament de Física Aplicada i Òptica, Av. Diagonal 647, E-08028 Barcelona, Spain

(Received 20 July 1998; accepted 13 September 1999)

Calcium phosphate coatings, obtained at different deposition rates by pulsed laser deposition with a Nd:YAG laser beam of 355 nm wavelength, were studied. The deposition rate was changed from 0.043 to 1.16 Å/shot by modification of only the ablated area, maintaining the local fluence constant to perform the ablation process in similar local conditions. Characterization of the coatings was performed by scanning electron microscopy, x-ray diffractometry, and infrared, micro-Raman, and x-ray photoelectron spectroscopy. The coatings showed a compact surface morphology formed by glassy grains with some droplets on them. Only hydroxyapatite (HA) and alpha-tricalcium phosphate (α–TCP) peaks were found in the x-ray diffractograms. The relative content of α–TCP diminished with decreasing deposition rates, and only HA peaks were found for the lowest rate. The origin of α–TCP is discussed.

I. INTRODUCTION

One approach to enhancing the biocompatibility of implants is to coat their surfaces with a biocompatible material. Such coatings increase the life of the implant and, if bioactive, they allow direct bonding between bone and implant and accelerate the process of healing and growth of bone. Calcium phosphates, especially hydroxyapatite (HA), are at the forefront of biomaterials due to their similarity to the inorganic component of bone. The different phases of calcium phosphate have different behavior when implanted in the body. Although HA is the most stable, other phases with lower stability are resorbed and offer a dynamic surface.

The deposition of HA coatings on titanium implants relied on the plasma-spray technique. It was not until the beginning of the nineties that pulsed laser deposition (PLD) was proposed as a new technique to improve the quality of the HA coatings.[1–4] The products of the laser–target interaction are atoms, molecules, small aggregates, and large particulates or droplets, with a high ratio of ions. By varying the laser beam characteristics and the nature of the target, the presence and proportion of these populations can be changed.[5,6] Two approaches have been pursued in order to obtain hydroxyapatite coatings by PLD. In one approach, the material from the target is mainly emitted in form of micrometer-size particulates that are collected at the substrate to form the film.[7,8] In the other approach, atoms, molecules, and small clusters are transferred from the target to grow the HA material.[1,9–12] The PLD technique allows reproducible production of coatings with different composition and phases and even with hydroxyapatite as the only phase. Thus a thorough study of the influence of the involved technological parameters on the properties of the coatings is required.

Although most of the research related to PLD of hydroxyapatite was based on the use of a KrF excimer laser ($\lambda = 248$ nm),[1,9–11,13] a ruby laser ($\lambda = 694$ nm) has also been used,[2,7,8] and good results have been obtained with an ArF excimer laser ($\lambda = 193$ nm).[4,11,12] Moreover, the fundamental wavelength of a Nd:YAG laser and its harmonics (1.064 μm, 355 nm, and 266 nm) have been used to ablate tricalcium phosphate with different absorptivities to study the relationship between the absorption of the target and the droplet areal density on the coatings.[14] Here we present for the first time a full characterization of films grown with a beam of wavelength 355 nm. The study is focused on revealing the role that the deposition rate plays on the synthesis of coatings with different calcium phosphate phases. The composition, structure, and morphology of the coatings were determined for different deposition rates, while the other parameters of the preparation process were fixed.

II. EXPERIMENTAL

The coatings were obtained by PLD using the third harmonic of a Nd:YAG laser ($\lambda = 355$ nm) operating at 10 Hz which gave pulses of 10 ns (full width half-

[a]Address all correspondence to this author.
e-mail: jmfernandez@fao.ub.es

maximum) and 0.28 J. The circular beam, with a Gaussian profile, was focused at 45° onto a target of HA with a density of 1.5 g/cm^3 made by compression of commercially available Merck powder with a Ca/P ratio of 1.7 measured by inductively coupled plasma. The spot had the shape of an ellipse whose semiaxis dimensions were 1.2 and 0.9 mm. The resulting fluence on the target surface was 7.8 J/cm^2. Usual methods to modify the deposition rate consist of using attenuators to diminish the fluence or changing the area of the focused spot leading to a modification of the fluence as well. Here, the deposition rate was lowered by placing metallic masks in the path of the beam to reduce the irradiated area but keeping the focus conditions to maintain a constant local fluence and thus performing the ablation process under similar local conditions. The coatings were grown on 2 × 2 cm^2 substrates of Ti–6Al–4V placed 4 cm in front of the target. Each deposition took 30 min, corresponding to 18,000 shots. All the coatings were made under an atmosphere of only H_2O at 45 Pa and the substrates were maintained at 530 °C during the process.

A stylus profiler revealed high values of surface roughness (up to 680 nm), which made it impossible to measure the thickness of the coatings accurately. The deposition rate was then determined by dividing the weight of each coating by its area and by the number of laser shots. In order to express the deposition rates in the more usual form, they were transformed to thickness per shot by assuming a density of 3.1 g/cm^3 for all the coatings. The deposition rates used were in the range of 0.043–1.16 Å/shot, or 0.43–11.6 Å s^{-1}. Thus the coatings had thicknesses in the range of 0.08–2.1 μm.

The phases in the coatings were analyzed by x-ray diffractometry (XRD). Fourier-transform infrared spectroscopy (FTIR) was used for the detection of hydroxyl groups in the apatite lattice and micro-Raman spectroscopy was used to find the spatial distribution of the phases. The stoichiometry of the coatings was evaluated by x-ray photoelectron spectroscopy (XPS). Their surface morphology was examined by scanning electron microscopy (SEM).

III. RESULTS AND DISCUSSION

Only two crystalline phases were detected in the XRD diffractograms of the coatings (Fig. 1): HA and alpha-tricalcium phosphate (α–TCP). There was no evidence for any preferential orientation. A first approximation to the relative content of these phases was evaluated from the ratio of the 170 peak of the α–TCP to the 211 peak of the HA (Fig. 2). The higher the deposition rate, the greater the relative content in α–TCP. Only HA peaks can be clearly identified in the diffractogram of the coating obtained at the lowest deposition rate. The background noise level does not allow ascertainment of the possible presence of α–TCP. Therefore, it seems beneficial to use low deposition rates when a coating of pure crystalline HA is required.

The morphology of all the coatings is quite similar (Fig. 3). They have a dense layer formed by grains of different sizes, on which isolated particulates or droplets are distributed. Most of them present a molten aspect; however, not all have a round shape as typical droplets. Their size distribution ranges from hundreds of nanometers to a few micrometers. An effect of coalescence is also noticed leading to bigger particles of irregular shape.

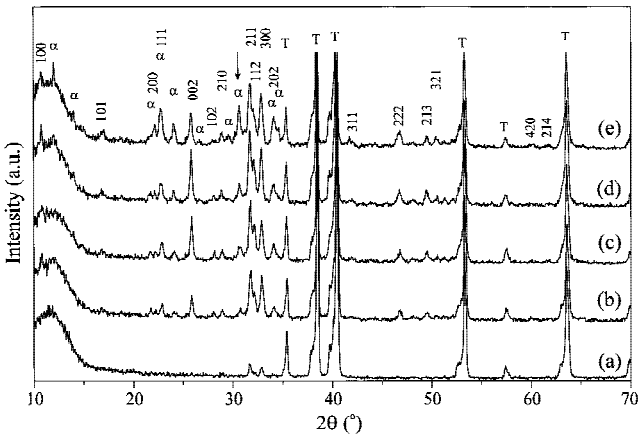

FIG. 1. X-ray diffractograms of coatings obtained at (a) 0.043 Å/shot, (b) 0.46 Å/shot, (c) 0.58 Å/shot, (d) 0.77 Å/shot, and (e) 1.16 Å/shot. Identified peaks correspond to HA. Peaks marked with α correspond to α–TCP and with T to Ti–6Al–4V. Arrow identifies the 170 peak of α–TCP.

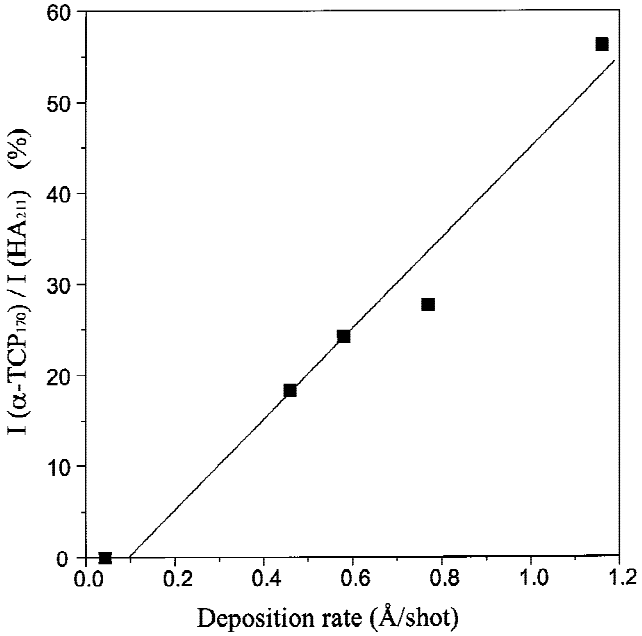

FIG. 2. Intensity ratio between the peaks 170 of α–TCP and 211 of HA of the x-ray diffractograms as a function of the deposition rate.

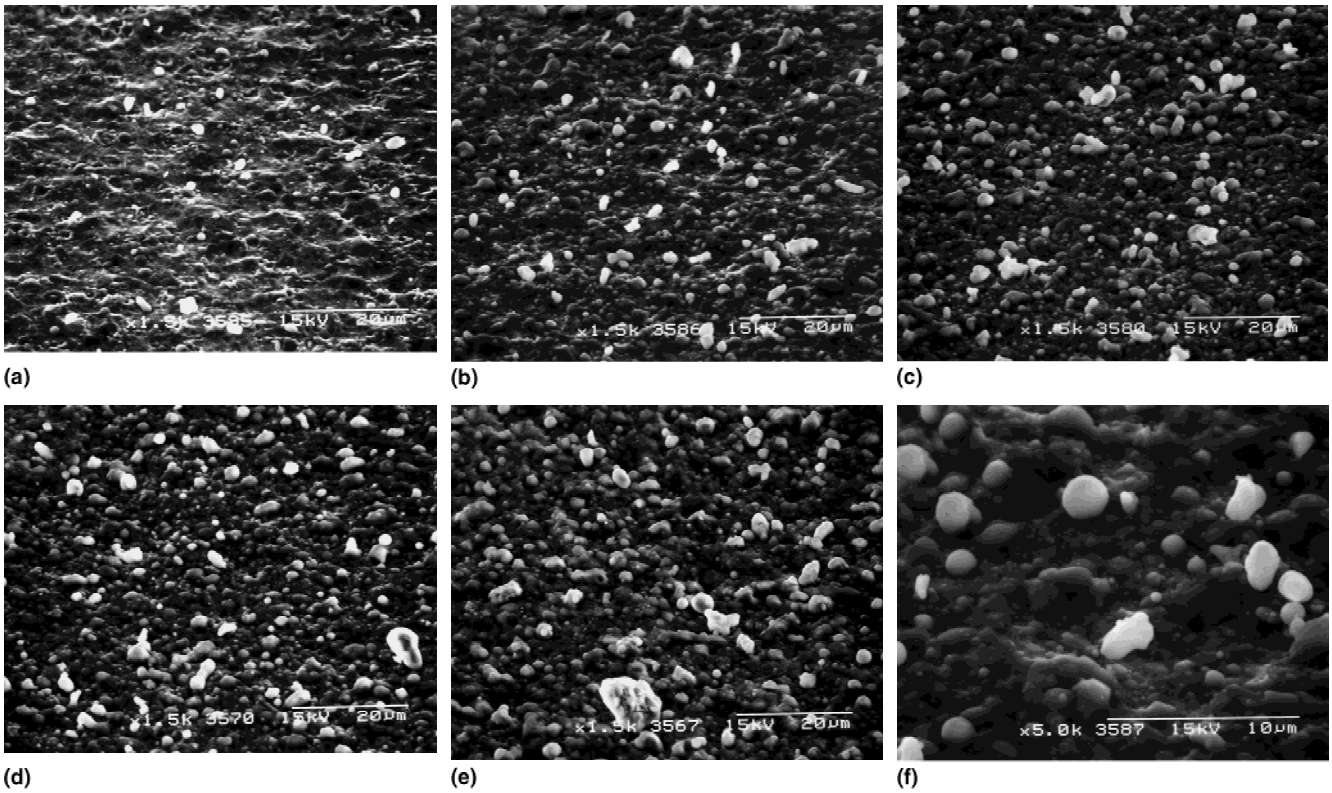

FIG. 3. SEM images of the coatings deposited at (a) 0.043 Å/shot, (b) 0.46 Å/shot, (c) 0.58 Å/shot, (d) 0.77 Å/shot, and (e) 1.16 Å/shot. (f) Higher magnification of the coating in (b).

Smoother surfaces are observed when using lower deposition rates. The coating deposited with the lowest deposition rate presents a low density of droplets, and this density increases with the deposition rate. This behavior is as expected because an increase in the deposition rate is only attributable to an increase of the ablated area, leading to a greater number of ejected particulates. The coatings present a specific morphology similar to those obtained with a ruby laser.[2,7,8] In contrast with coatings obtained with an excimer laser at similar conditions of temperature and atmosphere,[4,11] those obtained with the Nd:YAG laser have more droplets on their surface and present slightly glassy grains instead of elongated crystallites. This can be due to a lowering of the absorption coefficient of the HA targets at this higher wavelength, because it has been demonstrated that low absorption coefficients are directly related to the presence of more droplets on the coatings surface.[14] When using the excimer laser with shorter wavelengths, the droplet emission is reduced and the emission of atomic and molecular species is favored. The extreme case has been found at $\lambda = 193$ nm where no droplet emission is seen.[4,15]

The absence of bands attributable to carbonate groups in the FTIR spectra reveals that all the coatings are free from carbonate substitutions due to contamination. Also all the coatings spectra present the peaks characteristic of the hydroxyl groups. But on the thinnest coating, the stretching vibration of the hydroxyl group is masked by the vibrational band of the water absorbed superficially, which prevents its accurate quantification. The hydroxylation level had been estimated from the area of the deconvoluted peaks of the absorption spectra by comparing the content of hydroxyl groups to that of phosphate.[11] A greater incorporation of OH^- ions to the apatite lattice is favored by lower deposition rates (Fig. 4). Therefore, in this case the growth of the HA phase is enhanced in front of other phases free from these ions, like the tricalcium phosphates.

A semiquantitative analysis of the surface composition was performed by XPS. Lower Ca/P ratios are found for higher deposition rates (Fig. 5). The results are consistent with the phases identified by XRD, because α–TCP $[Ca_3(PO_4)_2]$ has a lower Ca/P ratio than HA $[Ca_{10}(PO_4)_6(OH)_2)]$. Nevertheless, these values cannot be taken as the real stoichiometry of the coatings because values obtained by means of the XPS technique do not always match with the real bulk stoichiometry.

Analyses performed by micro-Raman spectroscopy scanning each sample did not reveal differences between the spectra, indicating that there are no inhomogeneities in the phase distribution of the coatings, at least within a size equal to the analyzed spot area with a diameter of a micrometer.

Although the method used in this work to lower the deposition rate by reducing the ablated area may result in some changes in the ablation process, mainly due to heat diffusion processes, the use of masks minimizes these changes because no effects from changes in the local fluence are involved as for the usual methods. Taking into account that the local fluence is fixed and that at the lowest deposition rate only HA is detected as a crystalline phase, it can be considered that the content of α–TCP in the coatings is mainly related to processes occurring at the substrate and not to those occurring at the target. The results suggest that the amount of α–TCP is related to the rate of growth on the substrate. High growth rates would not allow complete crystallization in the HA-phase form and would favor the formation of α–TCP.

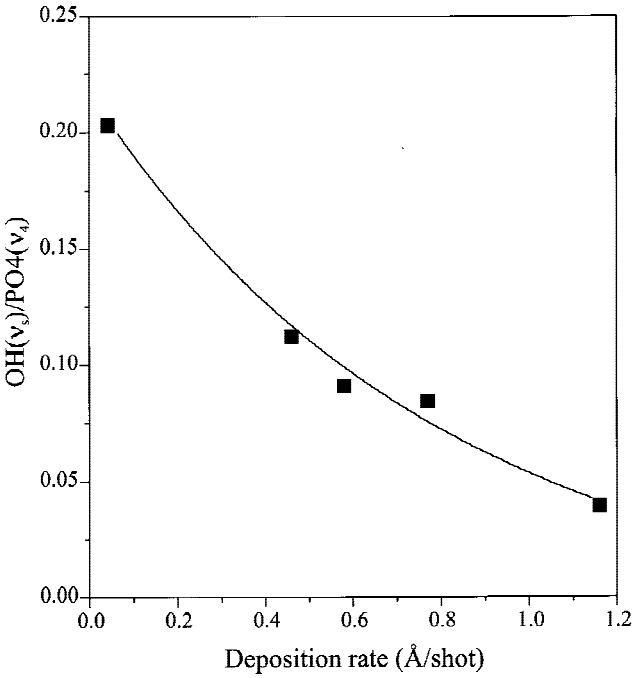

FIG. 4. Hydroxylation level, $OH\upsilon_s$ (3571 cm^{-1})/$PO_4\upsilon_4$ (band ~590 cm^{-1}), of the coatings as a function of the deposition rate.

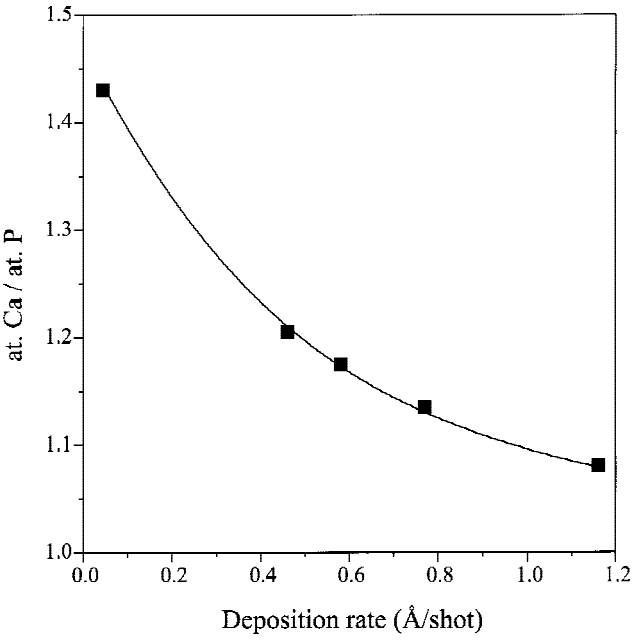

FIG. 5. Atomic calcium-to-phosphorus ratio evaluated by XPS as a function of the deposition rate.

Even though this explanation can be granted without objections, the presence of droplets in the coatings raises the question of their possible influence on the existence of the α–TCP phase. In order to study this possibility, a coating was deposited in the same conditions as the coating with the highest deposition rate, but with the substrate at room temperature. The x-ray diffractogram of this coating (Fig. 6) reveals that it is mainly amorphous. But over the glass bulge, some diffraction peaks of α–TCP and titanium phosphate hydroxide [$Ti(OH)PO_4$] can be identified. This α–TCP is assumed to come from the droplets, because it is the most stable phase at high temperatures below the melting point,[16] and a crystalline phase is unlikely to have grown from the small particles impinging on the substrate at room temperature, even although these particles were, as in the PLD process, highly energetic.

If the α–TCP phase forms in the droplets when the substrate is at room temperature, it may also be formed at higher temperatures, and at least some α–TCP in the coatings may thus come from the droplets. But could it be, moreover, that all of the α–TCP phase was in the droplets? To answer this question it should be taken into account that the ratio between droplets and other emitted particles should remain nearly constant for all the deposition rates. Nevertheless, the percentage of α–TCP in the coatings increases as the deposition rate increases.

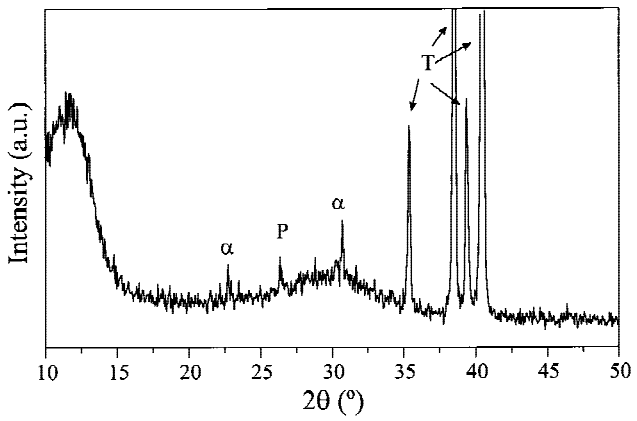

FIG. 6. X-ray diffractogram for an as-deposited coating obtained at room temperature. α = α–TCP, T = Ti–6Al–4V, and P = $Ti(OH)PO_4$.

Therefore, if the ratio of droplets would be maintained on the substrate, the increase of the α–TCP percentage with the deposition rate could not be explained solely by attributing the origin of α–TCP exclusively to the droplets.

IV. CONCLUSION

The surface morphology of the coatings obtained at the laser wavelength of 355 nm is different from that we have previously obtained with the shorter excimer laser wavelengths (193 and 248 nm). In the present case a compact layer formed by slightly glassy grains is observed and there is a higher density of droplets.

Increasing the deposition rate by increasing the ablated area at a constant local fluence leads to the production of coatings with higher contents of α–TCP. A coating containing only HA has been produced at a low deposition rate of 0.043 Å/shot.

Although the presence of α–TCP can be partly attributed to the droplets, the results suggest that the presence of α–TCP is related to the high rates of growth on the substrate.

ACKNOWLEDGMENTS

This work is a part of a program supported by CICYT of the Spanish Government (project MAT94-0264) and DGR of the Catalan Government.

REFERENCES

1. C.M. Cotell, D.B. Chrisey, K.S. Grabowski, J.A. Sprague, and C.R. Gossett, J. Appl. Biomater. **3,** 87 (1992).
2. P. Baeri, L. Torrisi, N. Marino, and G. Foti, Appl. Surf. Sci. **54,** 210 (1992).
3. G. Sardin, F. Sánchez, M. Varela, and J.L. Morena, Third European East-West Conference of E-MRS, Symposium on Biomaterials, Communication D-1.3, Strasbourg, France, 1992.
4. G. Sardin, M. Varela, and J.L. Morenza in *Hydroxyapatite and Related Materials*, edited by P.W. Brown and B. Constanz (CRC Press, London, 1994), p. 225.
5. P. Serra, J.M. Fernández-Pradas, G. Sardin, and J.L. Morenza, Appl. Surf. Sci. **109–110,** 384 (1997).
6. P. Serra and J.L. Morenza, J. Mater. Res. **13,** 1132 (1998).
7. L. Torrisi, Bio-Med. Mater. Eng. **3,** 43 (1993).
8. L. Torrisi, Thin Solid Films **237,** 12 (1994).
9. M. Jelínek, T. Dostálová, C. Fotakis, V. Studnicka, L. Jastrabik, V. Havránek, C. Grivas, V. Hnatowicz, J. Kadlec, A. Patentalaki, V. Perina, and M. Pospíchal, Laser Physics **6,** 144 (1996).
10. R.K. Singh, F. Qian, V. Nagabushnam, R. Damodaran, and B.M. Moudgil, Biomaterials **15,** 522 (1994).
11. J.M. Fernández-Pradas, G. Sardin, L. Clèries, P. Serra, C. Ferrater, and J.L. Morenza, Thin Solid Films **317,** 394 (1998).
12. F. García, J.L. Arias, B. Mayor, J. Pou, I. Rehman, J. Knowles, S. Best, B. León, M. Pérez-Amor, and W. Bonfield, J. Biomed. Mater. Res. (Appl. Biomater.) **43,** 69 (1998).
13. V.N. Bagratashvili, E.N. Antonov, E.N. Sobol, V.K. Popov and S.M. Howdle, Appl. Phys. Lett. **66,** 2451 (1995).
14. O. Guillot-Noël, R. Gomez-San Roman, J. Perrière, J. Hermann, V. Craciun, C. Boulmer-Leborgne, and P. Barboux, J. Appl. Phys. **80,** 1803 (1996).
15. P. Serra, L. Clèries, and J.L. Morenza, Appl. Surf. Sci. **96–98,** 216 (1996).
16. P.V. Riboud, Ann. Chim. **8,** 381 (1973).